Expanded View Figures

Figure EV1. RNA-seq analysis of sorted microglia.

A Volcano plot depicting the DEGs between the LPS and naïve groups. Dots represent non-DEGs (grey) and DEGs (FC > 0, red; FC < 0, blue); genes of interest were in dark colors.

B, C Bubble plots showing the top40 enriched suppressed/activated GO terms (B) as well as KEGG pathways (C) between the LPS and naïve groups.

D GSEA plot of the enriched KEGG pathways related to inflammation between the LPS and naïve groups.

E Category net plot of top5 enriched KEGG pathways when comparing the TPT group with the LPS group. The color gradient indicates the fold changes between the TPT and LPS groups computed by EdgeR (log2 transformed); the size of the category (pathways enriched) indicates the number of genes contributing to the enrichment.

F–H Heatmaps plotting the changes in expression levels of the genes contributing to the enrichment analysis of MAPK signaling pathway (F), Toll-like receptor signaling pathway (G), and IL-17 signaling pathway (H) across samples when comparing the TPT group with the LPS group.

I Bar plot of the 8 genes in (Fig 5I) according to BART result; Irwin-Hall *P*-value indicates the integrative rank significance; color gradients were coded by BART-computed relative rank.

J Bar plot of the *de novo* motifs enriched at the promoters of DEGs between the TPT and LPS groups; transcription factors with known motifs that matched the *de novo* motifs the best were listed accordingly.

© 2022 The Authors

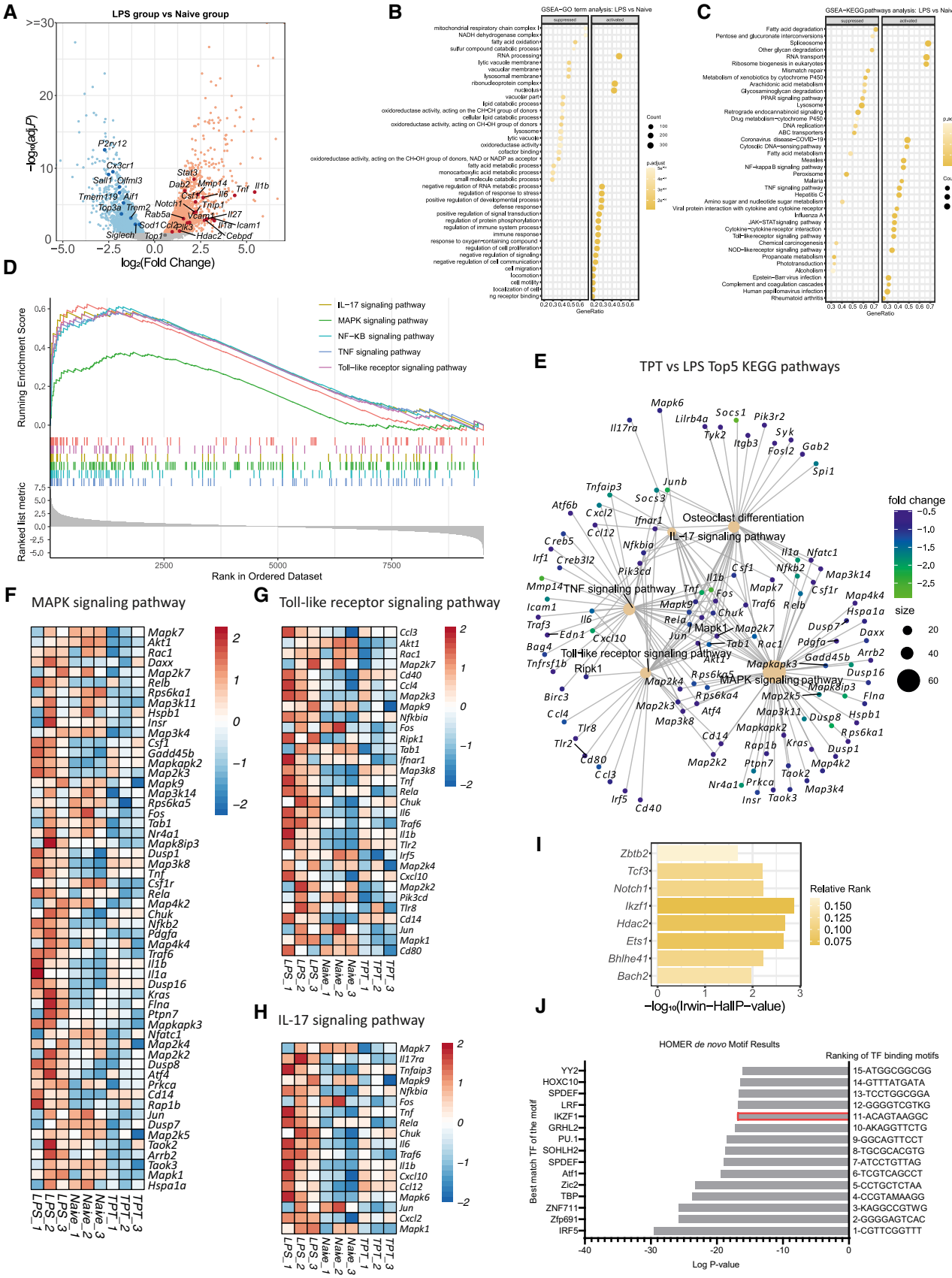

Figure EV1.

Figure EV2. Ikaros expression in activated macrophages/microglia and following TPT treatment.

A We analyzed a ChIP-seq dataset from Oh *et al* (2018a) (Data ref: Oh *et al*, 2018b) in which it profiled the genome-wide binding of Ikaros, encoded by the IKAROS Family Zinc Finger 1 (*Ikzf1*), in mouse macrophages before and after LPS treatment. We plotted the occupancy of Ikaros at the transcriptional start sites (TSS) of the 327 differentially expressed genes (DEGs) when comparing the TPT group with the LPS group, as well as of a random set of annotated genes with the same sample size as controls by using our RNA-seq data (Fig 5B). Ikaros occupancy at the TSS of DEGs was much higher when compared to the controls, and the binding of Ikaros at DEGs TSS sites increased after LPS treatment, indicating the close association between transcriptomic alteration caused by TPT treatment in the LPS model and Ikaros binding.

B mRNA expression of *Ikzf1* (normalized to *Gapdh* and *Hprt*)in adult mouse primary microglia following LPS/IFNɣ stimulation with or without TPT treatment after 4 or 8 h ($n = 3$ or 4 technical replicates).

C Representative immunofluorescent images showing Ikaros protein expression in mouse primary macrophages after 12 h LPS/IFNɣ stimulation with or without TPT treatment. Ikaros expression was displayed with a range indicator (white/gray), and the nuclei were stained with Hoechst (in blue); bar = 50 μm.

D Ikaros expression in the individual nucleus in (C) was quantified; 984, 1,186, and 1,145 nuclei were analyzed in the unstimulated, LPS/IFNɣ, and LPS/IFNɣ$^+$ TPT groups, respectively.

E, F Representative images showing the expression of Ikaros(in magenta) in the brain cortex in naïve mice and LPS challenged (4 h) mice with or without intracisternal TPT treatment (0.1 mg/kg); the brain sections were co-stained with microglia/macrophage antibodies P2RY12 and F4/80 (in green), and Hoechst (in blue). A magnified image from the yellow box in (E) was displayed in (F) with the arrows indicating the increased Ikaros expression in the nuclei of microglia/macrophages. Scale bar = 50 and 10 μmin (E) and (F), respectively.

G The semi-quantification of mean fluorescent intensity (MFI) of Ikaros in the cortex in (E); 2-6 sections from each mouse were analyzed.

Data information: Data are presented as the mean ± SEM. *$P < 0.05$; ***$P < 0.001$. Statistical analyses were performed using one-way ANOVA with Tukey's Multiple Comparison Test.

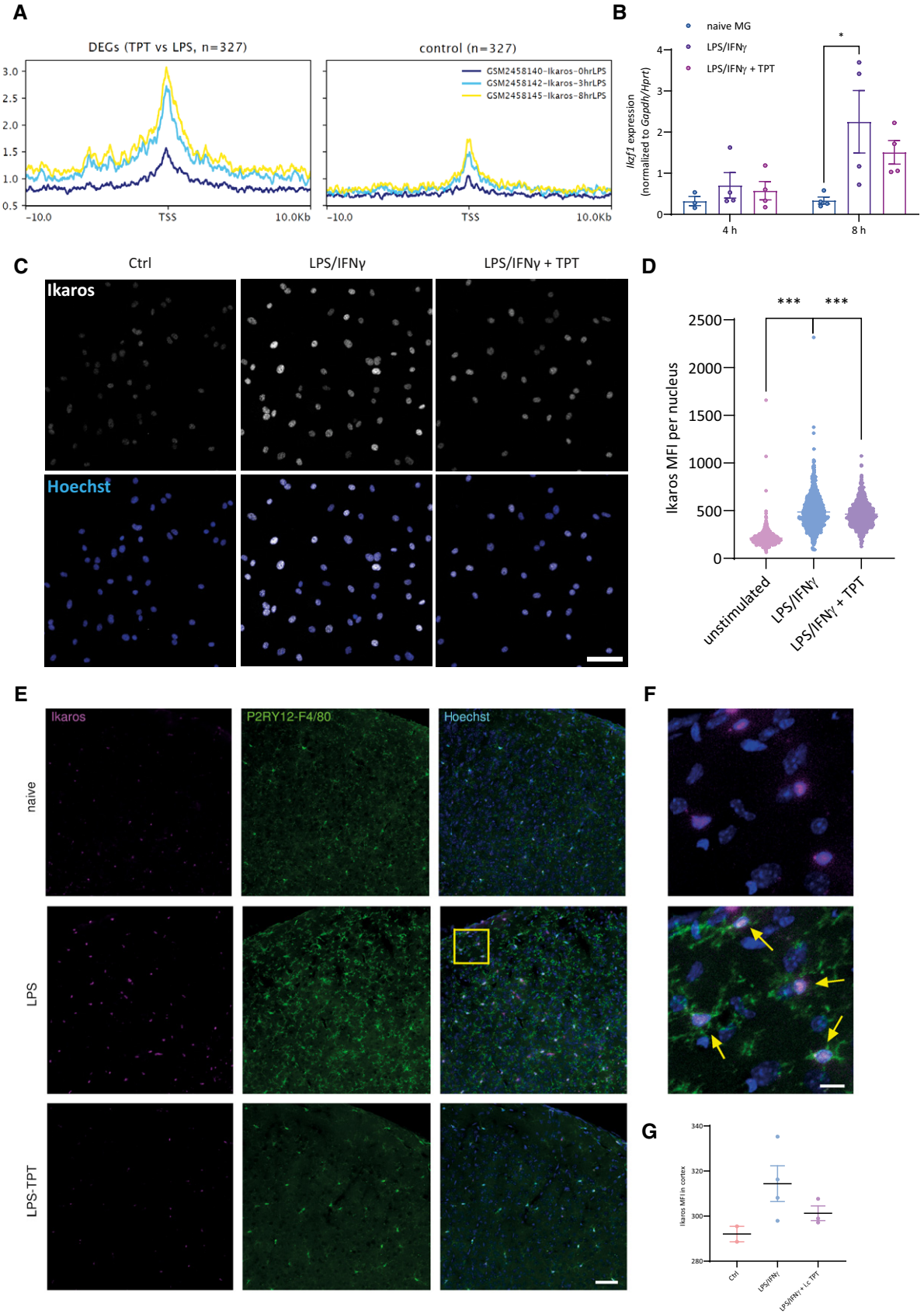

Figure EV2.

Figure EV3. Cytokine production of immune cells from EAE spinal cords at disease peak.

A, B Flow cytometry plots showing the production of IL-10 (A) and TNF-α (B) in the $CD11b^+$ myeloid cells; the frequency of IL-10-producing and TNF-α-producing $CD11b^+$ cells were graphed.

C, D The frequency of $Ki67^+$ $CD4^+$ T cells (C) and $Foxp3^+$ $CD4^+$ T cells (D) were graphed.

E, F The frequency of GM-CSF-producing (E) and IFN-γ-producing (F) $CD4^+$ cells was graphed.

Data information: Data are presented as the mean ± SEM. *$P < 0.05$ using the Student's unpaired two-tailed *t*-test; n.s. = no statistical significance; $n = 5$ and 7 biological replicates for the TPT group and the PBS group, respectively.

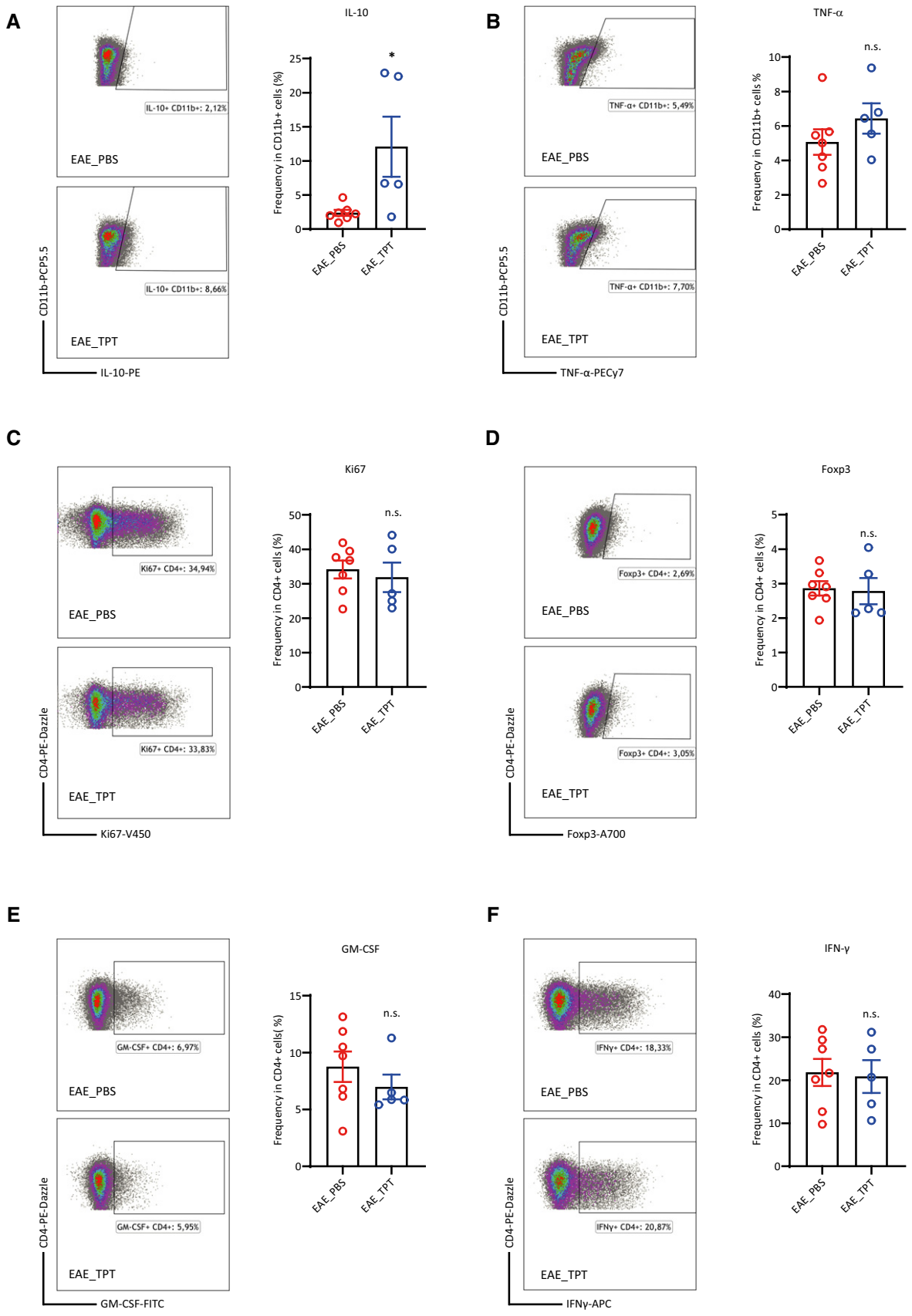

Figure EV3.

Figure EV4. MyloGami uptake *in vivo*.

A Mice received i.v injection of 100 μl 50 nM HR-Cy5 or MyloGami-Cy5 with 29 Cy5 sites per HR, or 100 μl saline with the same amount of Cy5 dissolved. Cy5 fluorescence distribution was imaged using an *in vivo* imaging system (IVIS-SpectrumCT) after 1, 2, 4, and 8 h.

B Mice received i.p injection of PBS (control) or 100 μl 50 nM MyloGami-Cy5, and the median fluorescent intensity (MFI) of Cy5 in myeloid cells, T cells, B cells and NK cells in the spleens were analyzed ($n = 2$ biological replicates for the control group, and $n = 6$ biological replicates for the MyloGami-Cy5 group) using flow cytometry 6 h after injection; the left panel represents the gating strategy. Data are presented as the mean ± SEM. *$P < 0.05$ when comparing the myeloid cells with any of the other cell types using one-way ANOVA with Tukey's Multiple Comparison Test.

C–E The liver (C) and kidney (D) sections of mice from (B) were stained with the macrophage marker F4/80 to evaluate the uptake of the Cy5 fluorescence in macrophages; bar = 50 μm; yellow arrows indicate representative colocalization of Cy5 fluorescence in the liver macrophages.D Mice received an intracisternal injection of 10 μl 100 nM MyloGami-Cy5, and after 3 h, the brain sections were stained with P2RY12 and F4/80 to label the myeloid cells in the brain (medulla oblongata); bar = 50 μm; yellow arrows indicate representative colocalization of Cy5 fluorescence in the CNS microglia/macrophages.

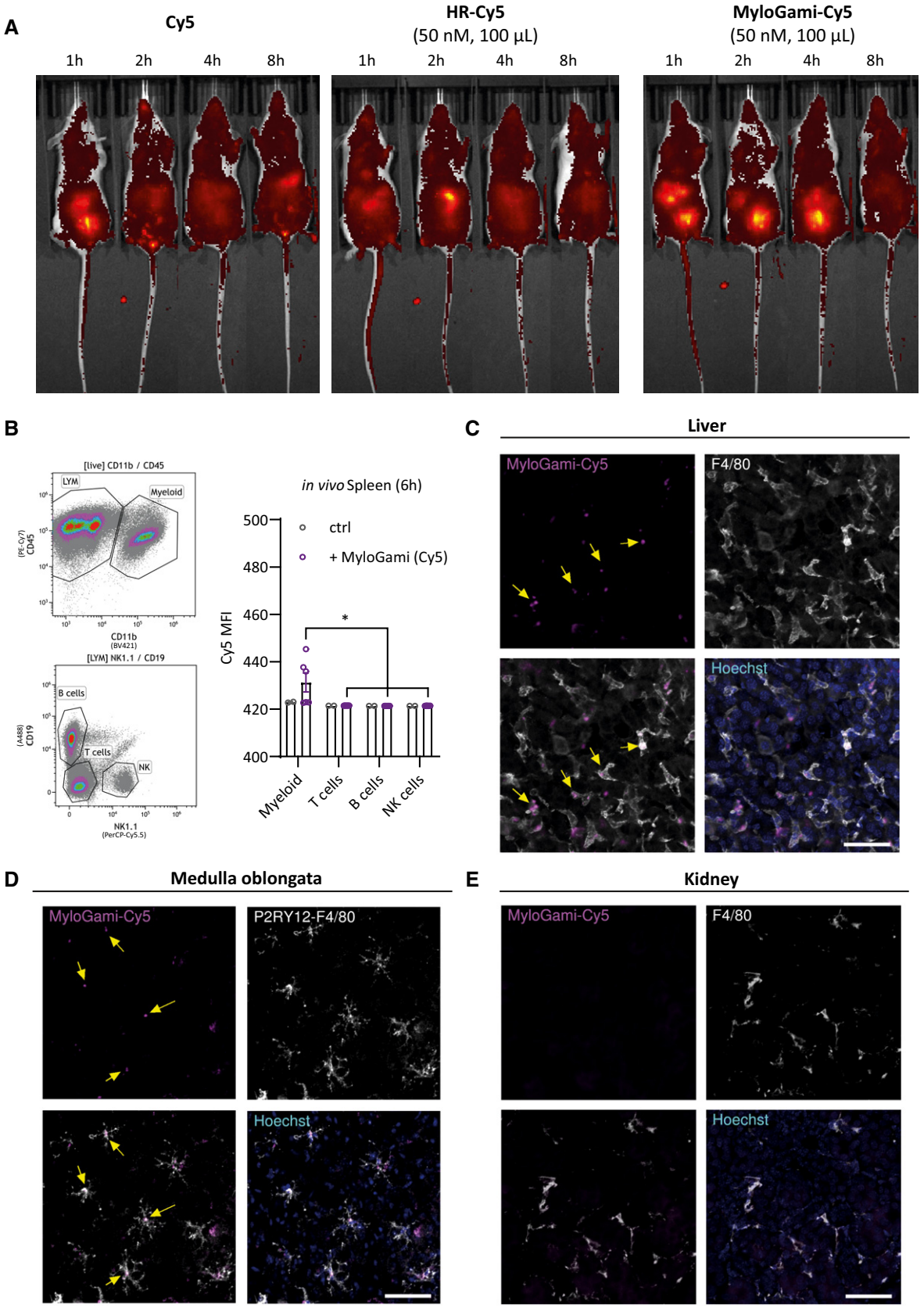

Figure EV4.

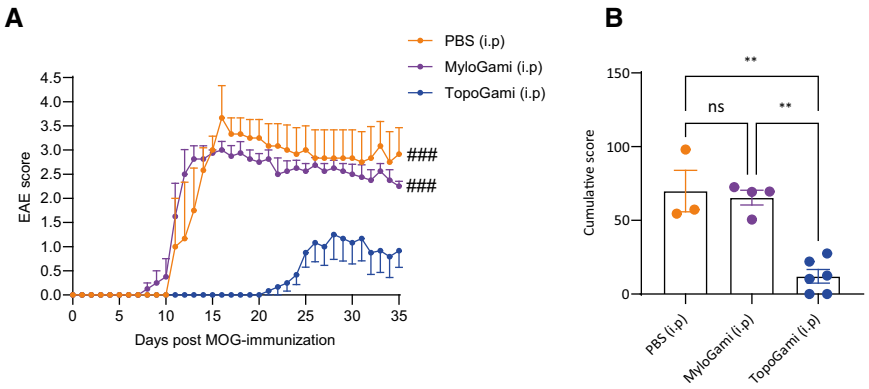

Figure EV5. TopoGami treatment (i.p) prevents EAE progression.

A TopoGami (or MyloGami/PBS controls) was administered to EAE mice on days 5, 7, and 9 post-immunization; the EAE clinical scores were graphed.

B Bar graph showing the cumulative EAE score in the 3 groups.

Data information: Data are presented as the mean ± SEM. $n = 3$–6 mice per group. $^{**}P < 0.01$ using Kruskal–Wallis nonparametric test for EAE cumulative score; ### $P < 0.001$ using one-way ANOVA with Tukey Multiple Comparisons Test for the area under the curve comparison of the EAE curves.